Article

Effect of the Preparation Conditions on the Magnetic Coercivity of CoPt Alloy Nanowires

Mihai Tibu, Nicoleta Lupu [ID] and Oana-Georgiana Dragos-Pinzaru *

National Institute of R&D for Technical Physics, 700050 Iasi, Romania
* Correspondence: odragos@phys-iasi.ro

Abstract: In this paper, 3 μm length and 200 nm diameter CoPt nanowire arrays (NWs) with different Co contents were prepared by electrodeposition at a controlled potential from an aqueous hexachloroplatinate solution. The synthesis occurred at two different solution pH values (2.5 and 5.5) in an electrochemical bath free of additives, as well as with saccharin as an organic additive. A complete morphological, compositional, structural and magnetic characterization of the as-prepared nanowires has been carried out. The results show that, by controlling the electrodeposition conditions, the Co content of the alloy can be tuned from 16% to 92%. The crystalline structure of the as-deposited compounds can also be controlled, with the obtained data showing that the face-centered cubic (fcc) crystalline structure changes into a hexagonal close-packed (hcp) structure when saccharin is used as an organic additive during the electrodeposition. The changes in the alloy's composition and crystalline structure strongly influence the magnetic properties of the NW's arrays.

Keywords: CoPt nanowires; electrodeposition; magnetic properties

1. Introduction

Nanotechnology and nanomaterials are the key elements for increasing the efficiency and performances of different devices and for developing new technologies in almost all domains of our lives, from medicine and healthcare (targeted drug delivery, regenerative medicine and diagnostics) to industry (information technology, electronics, textiles, cosmetics, environmental protection) and space exploration. Nanomaterials manifest novel physical and chemical properties compared with the properties of the same bulk or single-crystal materials, which are encouraging and promising for potential new applications or improving the existing technologies. In the last years, the synthesis, characterization and use of nanowires have been an emergent topic due to their unusual properties and the high surface-to-volume ratio of these materials [1–7]. The engineering of functionalized nanoparticles created for multimodal imaging or hyperthermia therapy and the optimization of their biological application are rapidly growing fields in nanomedicine. Despite the fact that iron oxide is currently one of the most commonly utilized magnetic nanoparticles for MRI contrast agents and for hyperthermia, CoPt and FePt with better magnetic characteristics may be new nano-objects with improved theranostic functions. Due to the clear connection between the atomic arrangement (surface segregation, strain, chemical order, etc.) and magnetic/catalytic performance, CoPt nanostructures are particularly intriguing systems.

One of the main goals of the research community is to prepare nanomaterials using easily controllable and less expensive fabrication techniques, such as electrochemical deposition, that do not require special logistics (including complex equipment such as high vacuum equipment, etc.). Among the metallic nanomaterials, nanowires based on noble (Pt) or transition metals (Co) are widely studied due to their potential applications in catalysis [8–11], biomedicine [12–15], magnetic recording (bit-patterned media) [16–22], MEMS (micro- and nano-electromechanical systems) [23], and sensors [24–29]. Future energy conversion and storage technologies, including water splitting [30,31], low-temperature

proton-exchange membrane fuel cells (PEMFC) [32,33], and metal–air batteries [34,35], will all rely heavily on electrocatalysis. Metallic nanostructured alloys are used in these applications because they enable an improvement in the reaction rate per unit of catalyst weight. However, improving the stability and efficiency of the electrocatalysts remains crucial; therefore, a fundamental advancement in their design is required. The well-known catalytic activity of Pt is counterbalanced by its high cost and scarcity; as a consequence, recent research is focused on reducing Pt usage by replacing it with non-noble and less expensive metals, such as Co, and improving, at the same time, its performances in applications as an electrocatalyst. Several preparation methods have been developed by researchers for the synthesis of CoPt alloys, such as thermal decomposition/reduction of organometallic precursors with a long-chain aliphatic diol, also known as the polyol process, the micellar technique, sol–gel methods and electrochemical deposition [36–39].

Using a potentiostatic electrodeposition approach, high-aspect-ratio magnetic nanowires with superior crystallinity and a faster growth rate could be electrodeposited inside alumina templates. Recently, in our laboratory, we have demonstrated the electrocatalytic performance of CoPt nanowires for the methanol oxidation reaction (MOR) [10] (up to 85 mAcm^{-2}), which has been increased even though the Pt content was lowered. CoPt alloys, manifesting optimized catalytic properties for the MOR with different compositions (ranging between 10% Pt and 90% Co), were obtained by controlling the preparation conditions.

The present study is intended to be a contribution to a better understanding of the magnetic properties of electrodeposited CoPt magnetic nanostructured alloys. Because they provide the possibility of fine-tuning the magnetic moments and the magnetic anisotropy energy by altering the composition and chemical order [40–42], CoPt nanostructures are one of the most interesting systems among nano-alloys due to their interesting magnetic properties, which are required for different applications, as was highlighted before. Magnetometry (using a superconducting quantum interference device (SQUID) or vibrating sample magnetometer (VSM), or based on magneto-optical Kerr effect (MOKE)) has been widely used to characterize Co–Pt nanostructures [43–45], being powerful techniques to study the magnetic properties (magnetic moment, anisotropy energy, etc.) of nano-alloys. The short- and long-range order of the alloys affects their various qualities. These ordering effects for the nanostructured alloys under consideration in this work have a direct impact on the magnetic properties of the alloy by changing its structural characteristics and chemical order (due to the direct link between atom arrangement and magnetic behavior). In this work, we performed global magnetometry using vibrating sample magnetometer (VSM) measurements to follow the magnetic behavior at room temperature and to study the magnetic properties of CoPt nanowires prepared under different conditions as a function of the Co content and the electrodeposition parameters.

The aim of this paper is to analyze the influence of the electrodeposition parameters during the preparation of CoPt nanowires on their magnetic properties. A special emphasis is given to the morphological, structural and compositional characterization. We also present an experimental analysis of the macroscopic magnetic properties.

2. Materials and Methods

The magnetic CoPt NWs were prepared by electrodeposition from a stable hexachloroplatinate CoPt aqueous solution containing 0.4 M H_3BO_3, 0.3 M NH_4Cl, 0.1 M $CoSO_4 \cdot 7H_2O$, 0.00386 M H_2PtCl_6, [46]. For the NW electrodeposition, two different solution pH values (2.5 and 5.5) were used. Additionally, during this work, hexachloroplatinate CoPt aqueous solution with and without saccharin as Na-salts as additives were used.

The electrodeposition was carried out into the nanopores of the anodic alumina template (AAO) provided by Whatman International Ltd., having a 25 mm diameter, a thickness of 40 μm and a nominal pore diameter of 200 nm. Prior to the electrodeposition, one side of the AAO template was covered with a thin layer of Ti (10 nm) and Cu (300 nm) (deposited by sputtering) in order to serve as the working electrode during the electrodeposition.

The electrochemical deposition of the CoPt alloys inside the alumina nanopores was performed by controlling the applied potential value. The electrochemical cell (having a volume of 100 mL) consists of a platinum wire as the counter electrode, an AAO template as the working electrode and a saturated calomel electrode (SCE) as the reference. The applied potential was controlled with a Heka potentiostat.

The electrodeposition was performed using different potential values ranging from -0.7 V/SCE to -1.0 V/SCE during an on-time of 2.5 s and a "rest" potential of -0.1 V/SCE during an off-time of 1 s. The off-time is necessary for a good "recovery" of the diffusion layer after the on-time when the electrodeposition occurs. Four sets of samples were prepared, as follows: two at solution pH value 2.5 (one in the absence of saccharin and the second in the presence of saccharin) and two at solution pH value 5.5 (also one in the absence of saccharin and the second in the presence of saccharin). Each sample set contains four different nanowire arrays obtained at -1 V, -0.9 V, -0.8 V, and -0.7 V, respectively.

Due to the fact that the nanowire growth rate is a function of the electrodeposition parameters, the electrodeposition rate was determined for each applied potential. It is well known that the magnetic properties of NWs are a function of their aspect ratio (ratio of length to width). Therefore, to compare the magnetic properties of NWs fabricated under different conditions, it is necessary to prepare samples with the same aspect ratio. In this work, we analyzed the magnetic properties of 3 μm long CoPt NWs, so the synthesis time was calculated for each applied potential before electrodeposition. It was found that the magnetic properties of NWs are greatly influenced by two parameters: the chemical composition of the alloy and the crystalline structure of the sample.

The as-prepared NW length and microstructure were observed by high-resolution—scanning electron microscopy (HR-SEM) using a CrossBeam System Carl Zeiss NEON40EsB. The elemental composition was determined by EDS measurements using the EDS facility of the same HR-SEM system. The magnetic properties were investigated by a vibrating sample magnetometer (VSM) using a Lake Shore VSM 7410 Vibrating Sample Magnetometer, while the crystalline structure of the electrodeposited NWs was studied by X-ray diffraction (XRD) by means of a Bruker AXS D8-Advance X-Ray Diffractometer with parallel optical geometry using Cu-Kα radiation (λ = 1.5406 Å).

3. Results and Discussion

3.1. Morphological and Compositional Characterization

The morphology, aspect ratio and composition of NWs are important parameters that need to be analyzed as their physical (e.g., magnetic) properties are strongly influenced by them. In order to prepare NWs with homogeneous and reproducible properties, an important request is to have very good control of the electrodeposition parameters. Additionally, the synthesis of NW arrays with a specified length involves the knowledge of the NW's growth speed. In this regard, prior to the synthesis of targeted 3 μm length NWs, the growth speed was determined in different experiments. After performing the electrodeposition inside the AAO nanopores, the cross-section of all the samples was analyzed by HR-SEM, with the results presented in Figure 1. The HR-SEM analysis of the electrodeposited NW arrays shows that the CoPt alloy is uniformly electrodeposited inside the nanoporous template for all the samples. Additionally, it was confirmed that the microstructure of the nanowires is a function only of the alumina nanochannel diameter and shape and does not vary with the electrodeposition parameters or electrodeposition bath composition. Figure 1 shows typical HR-SEM images of the AAO template cross-section filled with CoPt NWs electrodeposited at different potential values from the solution with saccharin at pH 5.5. As was mentioned previously, since the magnetic properties of the nanowires are a function of their aspect ratio, in this work, we calculated the electrodeposition time in order to prepare nanowires of the same length (the diameter of the nanowires depends on the template nanopores' diameter and not on the electrodeposition conditions). The measured diameter of the nanowire is 210 mn, while the measured sample lengths are 3 ± 0.4 μm.
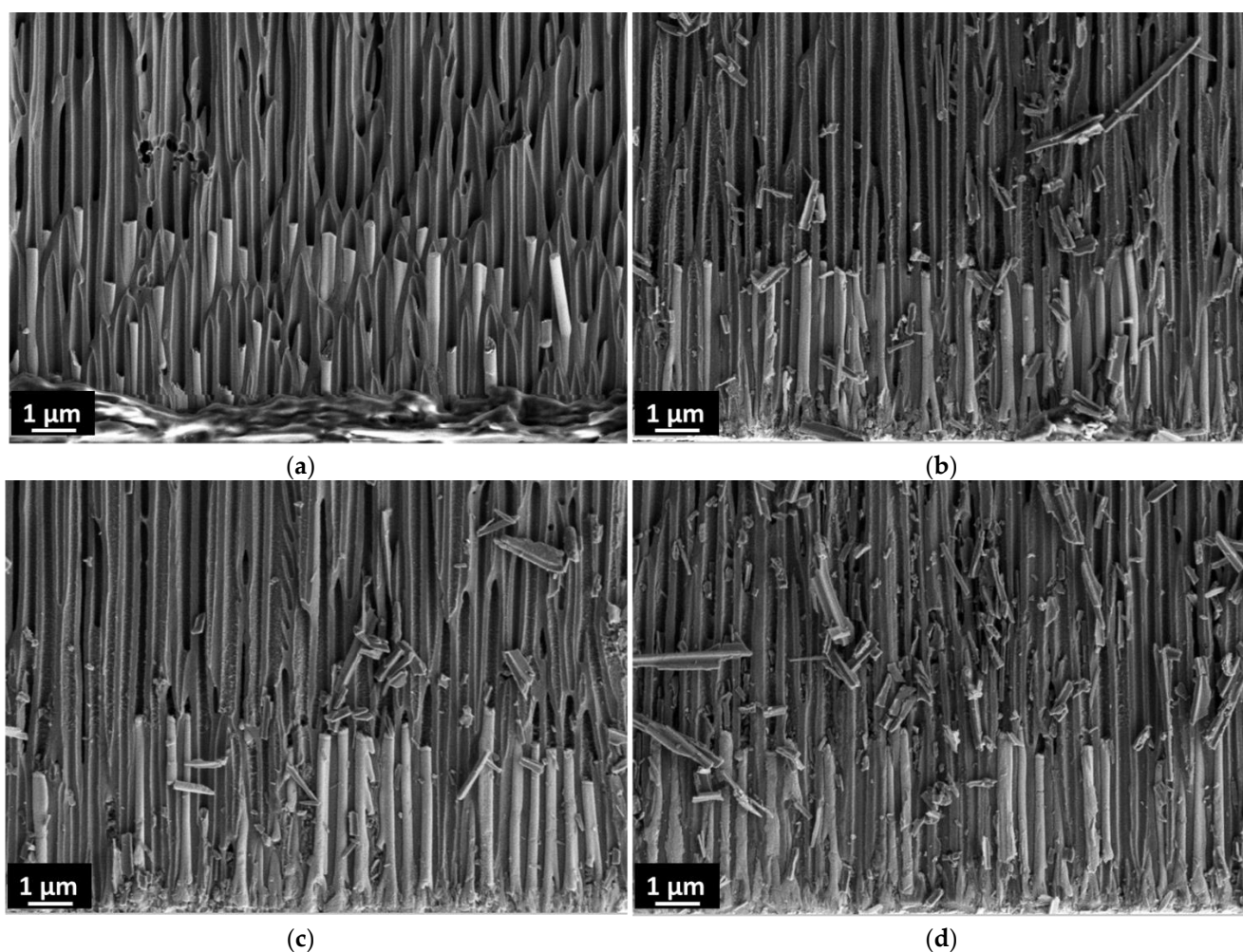
Figure 1. Cross-section HR-SEM image of CoPt nanowire arrays of 3.0 μm length prepared at different applied potentials: −0.7 V (**a**), −0.8 V (**b**), −0.9 V (**c**), −1.0 V (**d**).

The compositional analysis of the CoPt NWs performed by EDS establishes the presence of template elements (aluminum and oxygen) and the elements of the electrodeposited alloy (cobalt and platinum), showing the successful electrodeposition of the CoPt alloys inside the alumina template. However, the obtained compositional data (presented in Table 1) demonstrate that the alloy's content is substantially influenced by the applied potential and solution pH value.

Table 1. CoPt alloy composition determined by EDS measurements.

Applied Potential (V)	pH 2.5				pH 5.5			
	Without Sacch.		With Sacch.		Without Sacch.		With Sacch.	
	Co%	Pt%	Co%	Pt%	Co%	Pt%	Co%	Pt%
−0.7	16	84	37	63	35	65	40	60
−0.8	34	66	53	47	42	58	46	54
−0.9	44	56	73	27	66	34	77	23
−1.0	92	8	85	15	88	12	91	9

As can be observed from the table below, the chemical composition of the alloy can be tuned as a function of the electrodeposition parameters. Thus, CoPt alloys can be prepared with a Co content that varies from 16% to 92% by switching the potential value between −0.7 V/SCE and −1.0 V/SCE. Concerning the presence of additives during the

electrodeposition, the addition of saccharin leads to the preparation of magnetic NWs with a higher Co content for both pH values. A detailed description of the influence of the pH value and saccharin addiction on the alloy composition has been presented in our previous work [10].

The alloys' properties are strongly connected to their chemical composition, so it is very important to prepare materials having homogeneous compositions. In our previous work, we show the existence of a composition gradient in the CoPt thin films electrodeposited at a constant potential [2,47]. In order to avoid the apparition of a composition gradient along the nanowire's length, during this work, we establish (as we mentioned previously) a rest potential and time off. After setting these parameters, we prepared CoPt NW arrays having an NW length of 20 μm from the solution with saccharin at different pH values (2.5 and 5.5) and studied the composition along the nanowire's length by EDS. The electrodeposition was carried out by applying −1 V/SCE during the on-time of 2.5 s and 0.1 V/SCE during the off-time of 1 s. The SEM analysis (Figure 2a,c) shows the NWs are uniformly electrodeposited inside the alumina template, having uniform lengths, while the composition along the length of 20 μm NWs (presented in Figure 2b,d) was in the range of ±2% of the mean composition of CoPt.
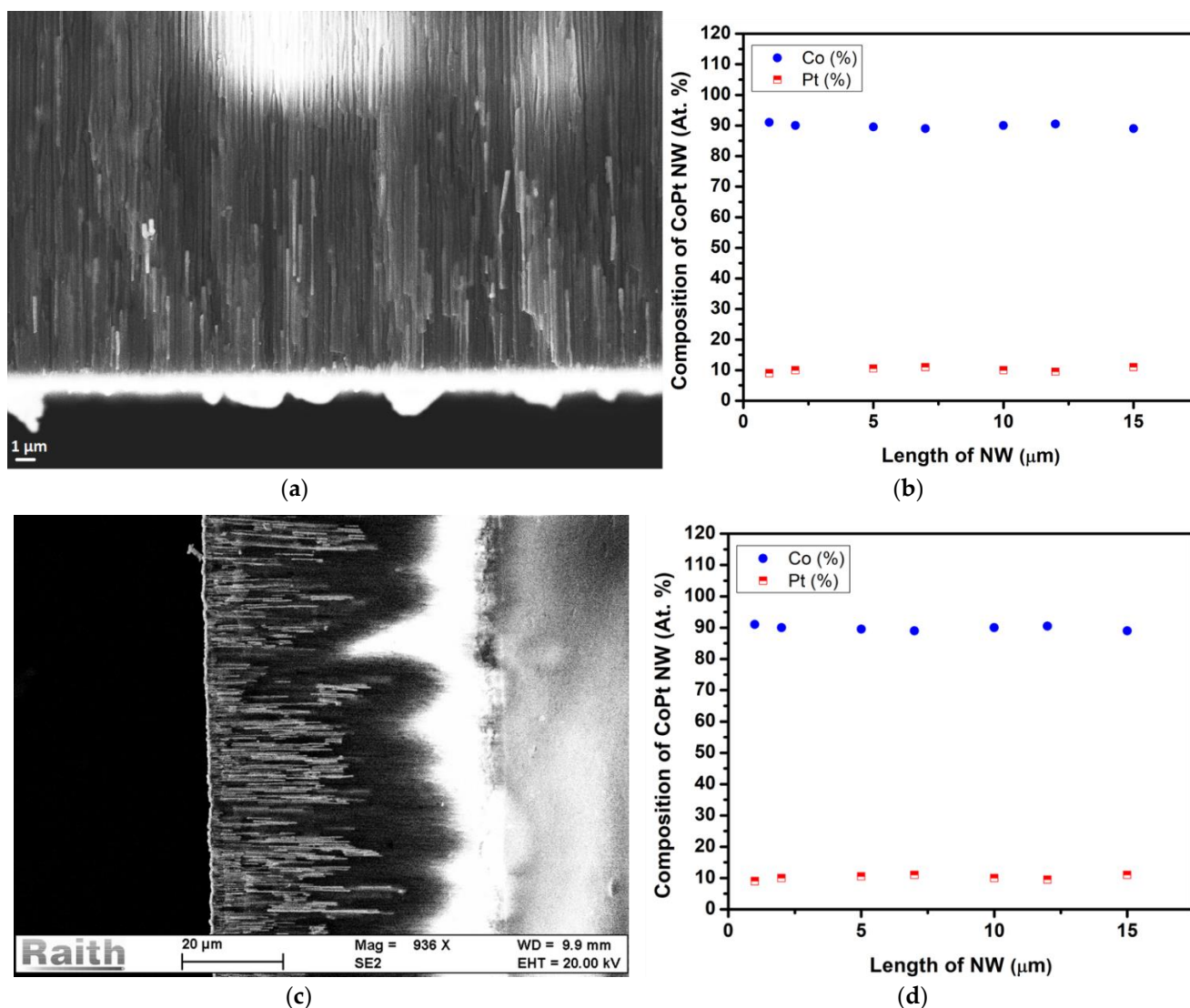

Figure 2. Cross-section SEM micrograph of CoPt NW array with 20 μm length prepared by applying −1.0 V from solution with saccharin at pH 2.5 (**a**) with the corresponding elemental composition (**b**) and at pH 5.5 (**c**) with the corresponding elemental composition (**d**), respectively.

3.2. Evolution of the Crystalline Structure of the CoPt NW's Function of the Solution pH and Organic Additive

The electrodeposition bath pH, as well as the presence of the organic additive, strongly influence the crystalline structure of the as-deposited CoPt NWs, as was previously demonstrated by our team [7]; the obtained results are presented in Figure 3.
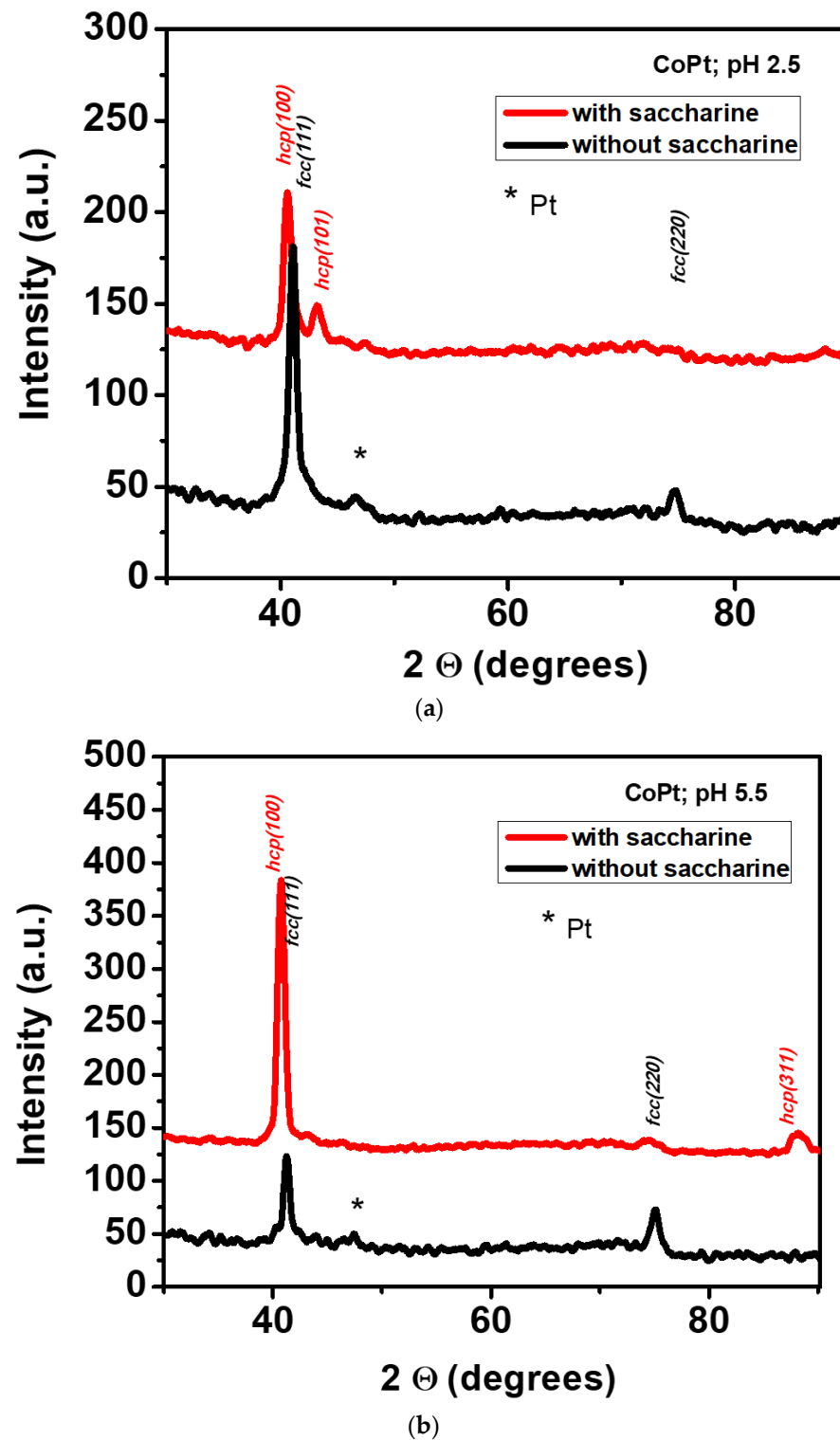

(a)

(b)

Figure 3. XRD patterns of CoPt nanowire arrays prepared from solution without additive (black curves) and with additive (red curves) at pH 2.5 (**a**) and 5.5 (**b**).

The XRD analysis shows that the CoPt NWs prepared from the solution free of additives present an fcc structure with a crystallite orientation along (111) and (220) fcc reflections, while the NWs prepared in the presence of additives exhibit an hcp structure having the predominant growth axis along the (100) reflection. However, small differences in crystallite orientation are visible on the diffractograms: the diffraction pattern of the NWs synthetized at pH 2.5 from solution with saccharin presents a (101) hcp reflection and, by increasing the solution pH from 2.5 at 5.5, the (101) reflection disappears, and a new diffraction peak characteristic of the hcp (311) reflection appears. As will be discussed further, the crystalline structure influences the magnetic properties of the as-prepared CoPt NWs.

3.3. Influence of the Preparation Conditions on the Magnetic Properties of the CoPt NWs

The magnetic properties of CoPt NWs prepared under different conditions were studied at room temperature as a function of the Co content and the electrodeposition parameters. The easy magnetization axis is perpendicular to the NW's growth axis for all the analyzed samples. The magnetic anisotropy of nanowire arrays is determined by four main contributions: the magnetocrystalline anisotropy, the shape anisotropy, the magnetostatic anisotropy and the magnetoelastic anisotropy. In Co-based nanowires, magnetoelastic anisotropy can be disregarded. Therefore, there is strong competition between the magnetocrystalline, magnetostatic and shape anisotropies in the magnetic nanowires. The first two anisotropies induce an easy magnetization axis perpendicular to the nanowire axis, depending on the crystalline phase and its growing direction, while the shape anisotropy determines an easy magnetization axis parallel to the nanowire length [48,49]. Since the aspect ratio of the nanowires is quite similar for the different studied compositions, and the nanowires have been deposited into the same type of templates, the contributions of shape anisotropy and magnetostatic anisotropy are expected to be the same for all samples. The variation of coercivity in our samples comes from the contribution of the magnetocrystalline anisotropy, which depends on the crystalline phase and its growing direction induced by the electrodeposition parameters.

Figure 4 shows the magnetic hysteresis loops of the CoPt NW arrays synthetized at −0.9 V from the electrochemical bath with and without saccharin as an organic additive at pH values of 2.5 and 5.5.

The values of the magnetic coercivities (Hc) for the magnetic field applied parallel and perpendicular to the NW's axis of the CoPt NWs prepared at pH 2.5 (solution with and without saccharin) and pH 5.5 (also with and without saccharin) as a function of the applied potential are presented in Table 2, while Figure 5 shows the variation in the magnetic coercivity values (Hc) depending on the alloys' Co content for the magnetic field applied parallel and perpendicular to the NW axis of the CoPt NWs prepared in a pH 2.5 solution without (Figure 5a) and with saccharin (Figure 5c) and a pH 5.5 solution without saccharin (Figure 5b) and with saccharin (Figure 5d).

Table 2. Magnetic properties of CoPt NWs.

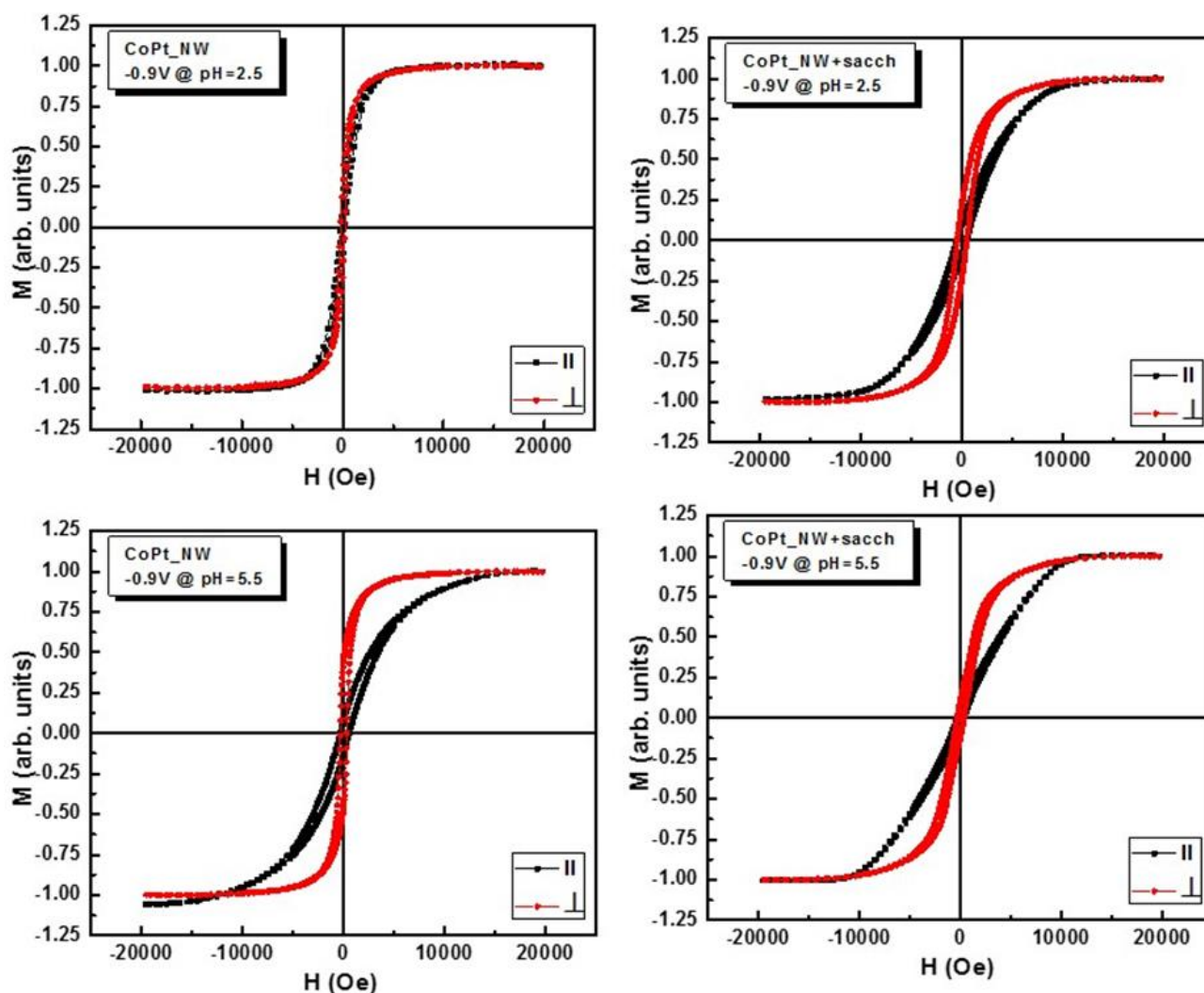| Applied Potential (V)	pH 2.5				pH 5.5			
	Paral. Coercivity (Oe)		Perp. Coercivity (Oe)		Paral. Coercivity (Oe)		Perp. Coercivity (Oe)	
	With Sacch.	Without Sacch.	With Sacch.	Without Sacch.	With Sacch.	Without Sacch.	With Sacch.	Without Sacch.
−0.7	222	26	263	26	150	41	166	34
−0.8	409	38.0	479	42.7	172	53	179	64
−0.9	454	176.3	481	221.7	412	320	333	323
−1.0	457	239.0	491	280.1	414	342	361	332

Figure 4. Hysteresis loops of the CoPt NW arrays electrodeposited by applying −0.9 V from electrochemical solution with different characteristics.

The magnetic properties are influenced by both the applied potential and the electrochemical bath composition. The shape of the magnetic hysteresis loops and the Hc values of the CoPt NWs show the competition between the shape anisotropy and crystallographic anisotropy. Our results show that, for the samples prepared from the electrochemical bath with the same characteristics (pH, presence/absence of additive), the Hc values increase with the increasing value of the applied potential. These results are in good accord with the EDS measurement: Co content in the alloy increases with the applied potential value. Additionally, the Hc value is higher for the samples prepared at the same pH and potential but in the presence of saccharin than those obtained from the solution without an additive. The highest Hc value was obtained for the NWs prepared in the presence of additives and at pH 2.5. All the samples from this batch manifest higher Hc values compared with those obtained at pH 5.5. The magnetic behavior of CoPt NWs is the result of two factors: (1) Co content and (2) the crystalline structure of the alloy. Considering these factors, the variation in the Hc value can be easily understood: the Hc increases with the increasing Co content of the sample and with the proportion of the hcp phase (hcp alloys manifest strong anisotropic behavior compared with fcc alloys). The increase in the coercivity for the samples obtained in presence of additives is the result of the fact that the Co content increases when additives are added as well as when the crystalline structure is changed. Nevertheless, the composition of the NWs prepared in the presence of saccharin slightly differs from those prepared from the solution without additives, but the Hc values are

different; specifically, they are higher for the samples prepared at smaller pH values. In this case, the magnetic properties are strongly influenced by the crystallographic structure of the CoPt alloy. As we showed previously, the addition of saccharin as an additive into the electrochemical bath leads to the change of the crystalline structure from cubic to hexagonal, but with a different crystal orientation function of the pH of the electrochemical bath. For our samples, despite the fact that the predominant crystalline orientation is the (100) axis, the small number of crystals oriented along the (311) axis present in the samples prepared at pH 5.5 in the presence of saccharin lead to the decrease in Hc values compared with the samples obtained from the solution at pH 2.5 in the same preparation conditions.
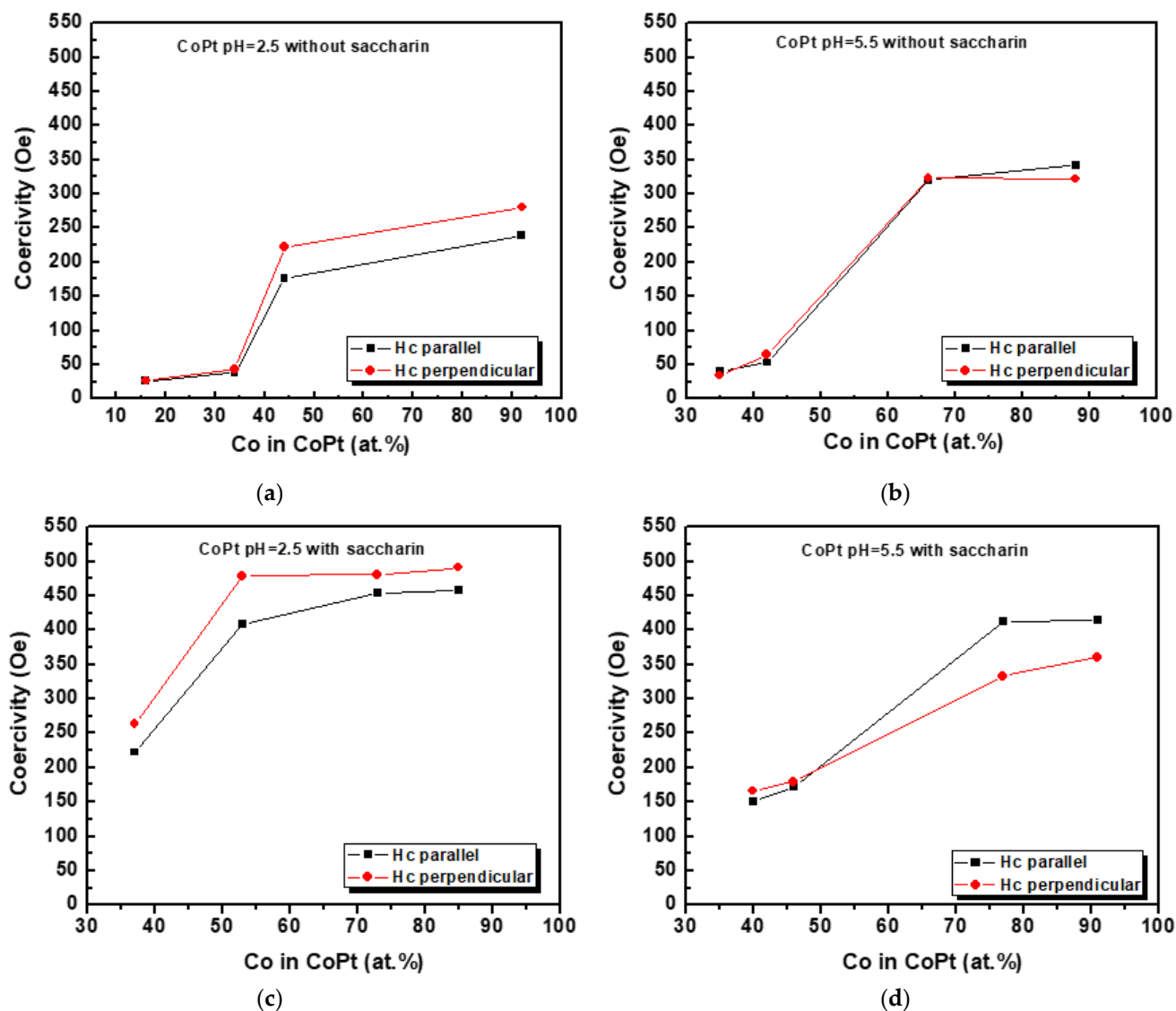

(a)

(b)

(c)

(d)

Figure 5. Variation of the magnetic coercivity values (Hc) depending on the alloys' Co content for the magnetic field applied parallel and perpendicular with the NW's axis of the CoPt NWs prepared in pH 2.5 solution without (**a**) and with saccharin (**c**) and pH 5.5 solution without saccharin (**b**) and with saccharin (**d**).

4. Conclusions

CoPt NWs with a 200 nm diameter and 3 μm length were obtained from a stable hexachloroplatinate solution by electrodeposition at a controlled potential. The electrochemical synthesis was carried out by electrodeposition in a sealed three-electrode cell from an electrochemical bath with and without saccharin at pH 2.5 and 5.5. It was demonstrated that the chemical composition of the as-deposited alloys is a function of the applied potential,

pH of the electrodeposition solution and presence of saccharin as an organic additive in the plating solution. Thus, the magnetic element concentration in the alloy can be tuned from 16% to 92% by adjusting the electrodeposition potential value and solution characteristics. The Co content is increased, at the same time, with the increase in the electrodeposition pH value. The same effect on the electrodeposited alloy composition was observed when saccharin was added to the electrochemical bath. The NW's composition remains stable during the electrodeposition process since no composition gradient was found along the nanowire's length in the present working conditions. The addition of saccharin into the electrochemical bath also has an important influence on the CoPt NW's crystalline structure as well as the crystallite orientation and, consequently, on the nanowire's magnetic behavior. Concerning the crystalline structure, the presence of saccharin in the plating solution favors the preparation of the hcp phase having a predominant crystalline orientation along the (100) axis. However, a small number of crystals are oriented along the (101) or (112) axis as a function of the electrodeposition bath pH. The change in the alloy structure is reflected in the magnetic properties: the coercive magnetic field increases when the saccharin is added to the electrochemical bath. The magnetic behavior of the CoPt NW arrays is discussed as a function of the plating solution pH, presence of additives and electrodeposition potential. It was found that the magnetic coercivity values (Hc) of the as-prepared nanowires depend on the alloy's Co content regardless of the direction of the applied magnetic field (parallel and perpendicular to the NW's axis).

Author Contributions: Conceptualization, O.-G.D.-P.; methodology, O.-G.D.-P., M.T., N.L.; formal analysis, O.-G.D.-P., M.T., N.L.; investigation, O.-G.D.-P., M.T., N.L.; resources, O.-G.D.-P.; writing—original draft preparation, O.-G.D.-P., M.T.; writing—review and editing, O.-G.D.-P., M.T.; supervision, O.-G.D.-P.; project administration, O.-G.D.-P.; funding acquisition, O.-G.D.-P. All authors have read and agreed to the published version of the manuscript.

Institutional Review Board Statement: Not applicable.

Informed Consent Statement: Not applicable.

Data Availability Statement: Not applicable.

Conflicts of Interest: The authors declare no conflict of interest.

References

1. Aricò, A.S.; Bruce, P.; Scrosati, B.; Tarascon, J.-M.; van Schalkwijk, W. Nanostructured materials for advanced energy conversion and storage devices. *Nat. Mater.* **2005**, *4*, 366–377. [CrossRef]
2. Tabakovic, I.; Qiu, J.-M.; Dragos, O. Electrodeposition of thin CoPt films with very high perpendicular anisotropy from hexachloroplatinate solution: Effect of saccharin additive and electrode substrate. *J. Electrochem. Soc.* **2016**, *163*, D287–D294. [CrossRef]
3. Ghemes, A.; Dragos-Pinzaru, O.; Chiriac, H.; Lupu, N.; Grigoras, M.; Shore, D.; Stadler, B.; Tabakovic, I. Controlled electrodeposition and magnetic properties of Co35Fe65 nanowires with high saturation magnetization. *J. Electrochem. Soc.* **2017**, *164*, D13–D22. [CrossRef]
4. Cortés, M.; Gómez, E.; Vallés, E. Electrochemical growth of CoPt nanowires of different aspect ratio and their magnetic properties. *J. Electroanal. Chem.* **2013**, *689*, 69–75. [CrossRef]
5. Inwati, G.K.; Rao, Y.; Singh, M. In Situ Free Radical Growth Mechanism of Platinum Nanoparticles by Microwave Irradiation and Electrocatalytic Properties. *Nanoscale Res. Lett.* **2016**, *11*, 458. [CrossRef]
6. Inwati, G.K.; Kumar, P.; Singh, M.; Yadav, V.K.; Kumar, A.; Soma, V.R.; Swart, H.C. Study of photoluminescence and nonlinear optical behaviour of AgCu nanoparticles for nanophotonics. *Nano-Struct. Nano-Objects* **2021**, *28*, 100807. [CrossRef]
7. Malik, P.; Inwati, G.K.; Mukherjee, T.K.; Singh, S.; Singh, M. Green silver nanoparticle and Tween-20 modulated pro-oxidant to antioxidant curcumin transformation in aqueous CTAB stabilized peanut oil emulsions. *J. Mol. Liq.* **2019**, *291*, 111252. [CrossRef]
8. Serrà, A.; Montiel, M.; Gómez, E.; Vallés, E. Electrochemical Synthesis of Mesoporous CoPt Nanowires for Methanol Oxidation. *Nanomaterials* **2014**, *4*, 189–202. [CrossRef]

9. Lu, Q.; Sun, L.; Zhao, X.; Huang, J.; Han, C.; Yang, X. One-pot synthesis of interconnected $Pt_{95}Co_5$ nanowires with enhanced electrocatalytic performance for methanol oxidation reaction. *Nano Res.* **2018**, *11*, 2562–2572. [CrossRef]

10. Dragos-Pinzaru, O.-G.; Stoian, G.; Borza, F.; Chiriac, H.; Lupu, N.; Tabakovic, I.; Stadler, B.J.H. CoPt Nanowires with Low Pt Content for the Catalytic Methanol Oxidation Reaction (MOR). *ACS Appl. Nano Mater.* **2022**, *5*, 8089–8096. [CrossRef]

11. Liu, H.; Li, C.; Chen, D.; Cui, P.; Ye, F.; Yang, J. Uniformly dispersed platinum-cobalt alloy nanoparticles with stable compositions on carbon substrates for methanol oxidation reaction. *Sci. Rep.* **2017**, *7*, 11421. [CrossRef]

12. Harish, V.; Tewari, D.; Gaur, M.; Yadav, A.B.; Swaroop, S.; Bechelany, M.; Barhoum, A. Review on Nanoparticles and Nanostructured Materials: Bioimaging, Biosensing, Drug Delivery Tissue Engineering, Antimicrobial, and Agro-Food Applications. *Nanomaterials* **2022**, *12*, 457. [CrossRef]

13. Meng, X.; Seton, H.C.; Lu, L.T.; Prior, I.A.; Thanh, N.T.K.; Song, B. Magnetic CoPt nanoparticles as MRI contrast agent for transplanted neural stem cells detection. *Nanoscale* **2011**, *3*, 977–984. [CrossRef]

14. Fang, X.; Zhao, X.; Fang, W.; Chen, C.; Zheng, N. Self-templating synthesis of hollow mesoporous silica and their applications in catalysis and drug delivery. *Nanoscale* **2013**, *5*, 2205–2218. [CrossRef]

15. Contreras, M.; Sougrat, R.; Zaher, A.; Ravasi, T.; Kosel, J. Nonchemotoxic induction of cancer cell death using magnetic nanowires. *Int. J. Nanomed.* **2015**, *10*, 2141–2153. [CrossRef]

16. Shamaila, S.; Sharif, R.; Riaz, S.; Ma, M.; Khaleeq-ur-Rahman, M.; Han, X.-F. Magnetic and magnetization properties of electrodeposited fcc CoPt nanowire arrays. *J. Magn. Magn. Mater.* **2008**, *320*, 1803–1809. [CrossRef]

17. Cortés, M.; Serrà, A.; Gómez, E.; Vallés, E. CoPt nanoscale structures with different geometry prepared by electrodeposition for modulation of their magnetic properties. *Electrochim. Acta* **2011**, *56*, 8232–8238. [CrossRef]

18. Franz, S.; Bestetti, M.; Cavallotti., P.L. Co–Pt thin films for magnetic recording by ECD from acidic electrolytes. *J. Magn. Magn. Mater.* **2007**, *316*, e173–e176. [CrossRef]

19. Sirtori, V.; Cavallotti, P.L.; Rognoni, R.; Xu, X.; Zangari, G.; Fratesi, G.; Trioni, M.I.; Bernasconi, M. Unusually large magnetic anisotropy in electrochemically deposited Co-rich Co-Pt films. *ACS Appl. Mater. Interfaces* **2011**, *3*, 1800–1803. [CrossRef]

20. Cortés, M.; Gómez, E.; Vallés, E. Magnetic CoPt (60–70 wt% Pt) microstructures fabricated by the electrochemical method. *J. Micromech. Microeng.* **2012**, *22*, 055016. [CrossRef]

21. Meneses, F.; Bran, C.; Vázquez, M.; Bercoff, P.G. Enhanced in plane magnetic anisotropy in thermally treated arrays of Co-Pt nanowires. *Mater. Sci. Eng. B* **2020**, *261*, 114669. [CrossRef]

22. Cavallotti, P.L.; Bestetti, M.; Franz, S. Microelectrodeposition of Co−Pt alloys for micromagnetic applications. *Electrochim. Acta* **2003**, *48*, 3013–3020. [CrossRef]

23. Rochaz, L.V.; Dieppedale, C.; Desloges, B.; Gamet, D.; Barragatti, C.; Rostaing, H.; Meunier-Carus, J. Electrodeposition of hard magnetic CoPtP material and integration into magnetic MEMS. *J. Micromech. Microeng.* **2006**, *16*, 219–224. [CrossRef]

24. Sharma, M.K.; Kuanr, B.; Sharma, M.; Basu, A. New opportunities in microwave electronics with ferromagnetic nanowires. *J. Appl. Phys.* **2014**, *115*, 17A518. [CrossRef]

25. Cavallotti, P.L.; Bucher, P.; Lecis, N.; Zangari, G. Microstructure and magnetic properties of electrodeposited CoPt and CoPtP alloy thin films. *Electrochem. Soc. Proc.* **1998**, *95*, 169–180.

26. Skomski, R.; Zeng, H.; Zheng, M.; Sellmyer, D.J. Magnetic localization in transition-metal nanowires. *Phys. Rev. B* **2000**, *62*, 3900–3904. [CrossRef]

27. Dahmane, Y.; Cagnon, L.; Voiron, J.; Pairis, S.; Bacia, M.; Ortega, L.; Benbrahim, N.; Kadri, A. Magnetic and structural properties of electrodeposited CoPt and FePt nanowires in nanoporous alumina templates. *J. Phys. D Appl. Phys* **2006**, *39*, 4523–4528. [CrossRef]

28. Darques, M.; la Torre Medina, J.D.; Piraux, L.; Cagnon, L.; Huynen, I. Microwave circulator based on ferromagnetic nanowires in an alumina template. *Nanotechnology* **2010**, *21*, 145208. [CrossRef]

29. Gandha, K.; Elkins, K.; Poudyal, N.; Liu, X.; Liu, J.P. High energy product developed from cobalt nanowires. *Sci. Rep.* **2014**, *4*, 5345. [CrossRef]

30. Anwar, S.; Khan, F.; Zhang, Y.; Djire, A. Recent development in electrocatalysts for hydrogen production through water electrolysis. *Int. J. Hydrogen Energy* **2021**, *46*, 32284–32317. [CrossRef]

31. Cavaliere, P.D.; Perrone, A.; Silvello, A. Water Electrolysis for the Production of Hydrogen to Be Employed in the Ironmaking and Steelmaking Industry. *Metals* **2021**, *11*, 1816. [CrossRef]

32. Zhao, X.; Sasaki, K. Advanced Pt-Based Core–Shell Electrocatalysts for Fuel Cell Cathodes. *Acc. Chem. Res.* **2022**, *55*, 1226–1236. [CrossRef] [PubMed]

33. Alink, R.; Singh, R.; Schneider, P.; Christmann, K.; Schall, J.; Keding, R.; Zamel, N. Full Parametric Study of the Influence of Ionomer Content, Catalyst Loading and Catalyst Type on Oxygen and Ion Transport in PEM Fuel Cell Catalyst Layers. *Molecules* **2020**, *25*, 1523. [CrossRef] [PubMed]

34. Wang, L.; Snihirova, D.; Deng, M.; Vaghefinazari, B.; Xu, W.; Höche, D.; Lamaka, S.V.; Zheludkevich, M.L. Sustainable aqueous metal-air batteries: An insight into electrolyte system. *Energy Storage Mater.* **2022**, *52*, 573–597. [CrossRef]

35. Olabi, A.G.; Sayed, E.T.; Wilberforce, T.; Jamal, A.; Alami, A.H.; Elsaid, K.; Rahman, S.M.A.; Shah, S.K.; Abdelkareem, M.A. Metal-Air Batteries—A Review. *Energies* **2021**, *14*, 7373. [CrossRef]

36. Frommen, C.; Rösner, H.; Fenske, D. Wet-chemical synthesis and properties of CoPt and CoPt3 alloy nanoparticles. *J. Nanosci. Nanotechnol.* **2002**, *2*, 509. [CrossRef] [PubMed]

37. Mandal, M.; Das, B.; Mandal, K. Synthesis of Co(x)Pt(1-x) alloy nanoparticles of different phase by micellar technique and their properties study. *J. Colloid Interface Sci.* **2009**, *335*, 40. [CrossRef]

38. Liu, Y.; Yang, Y.; Zhang, Y.; Wang, Y.; Zhang, X.; Jiang, Y.; Wei, M.; Liu, Y.; Liu, X.; Yang, J. A facile route to synthesis of CoPt magnetic nanoparticles. *Mater. Res. Bull.* **2013**, *48*, 721. [CrossRef]

39. Cagnon, L.; Dahmane, Y.; Voiron, J.; Pairis, S.; Bacia, M.; Ortega, L.; Benbrahim, N.; Kadri, A. Electrodeposited CoPt and FePt alloys nanowires. *J. Magn. Magn. Mater.* **2007**, *310*, 2428. [CrossRef]

40. Shuttleworth, I. The Magnetic Band-Structures of Ordered Pt_xFe_{1-x}, Pt_xCo_{1-x}, and Pt_xNi_{1-x} (x = 0.25, 0.50, and 0.75). *Magnetochemistry* **2020**, *6*, 61. [CrossRef]

41. Andreazza, P.; Pierron-Bohnes, V.; Tournus, F.; Andreazza-Vignolle, C.; Dupuis, V. Structure and order in cobalt/platinum-type nanoalloys: From thin films to supported clusters. *Surf. Sci. Rep.* **2015**, *70*, 188–258. [CrossRef]

42. Alam, A.; Kraczek, B.; Johnson, D.D. Structural, magnetic, and defect properties of Co-Pt-type magnetic-storage alloys: Density-functional theory study of thermal processing effects. *Phys. Rev. B* **2010**, *82*, 024435. [CrossRef]

43. Ersen, O.; Parasote, V.; Pierron-Bohnes, V.; Cadeville, M.C.; Ulhaq-Bouillet, C. Growth conditions to optimize chemical order and magnetic properties in molecular-beam-epitaxy-grown CoPt/MgO(001) thin films. *J. Appl. Phys.* **2003**, *93*, 2987–2995. [CrossRef]

44. Grange, W.; Galanakis, I.; Alouani, M.; Maret, M.; Kappler, J.-P.; Rogalev, A. Experimental and theoretical x-ray magnetic-circular-dichroism study of the magnetic properties of CoPt thin films. *Phys. Rev. B* **2000**, *62*, 1157. [CrossRef]

45. Dragos-Pinzaru, O.-G.; Buema, G.; Gherca, D.; Tabakovic, I.; Lupu, N. Effect of the Preparation Conditions on the Catalytic Properties of CoPt for Highly Efficient 4-Nitrophenol Reduction. *Materials* **2022**, *15*, 6250. [CrossRef]

46. Tabakovic, I.; Qiu, J.-M.; Riemer, S. Electrodeposition of CoPt Alloys from the Stable Hexachloroplatinate Solution: Electrochemical Studies. *J. Electrochem. Soc.* **2015**, *162*, D291–D299. [CrossRef]

47. Dragos-Pinzaru, O.; Ghemes, A.; Chiriac, H.; Lupu, N.; Grigoras, M.; Riemer, S.; Tabakovic, I. Magnetic properties of CoPt thin films obtained by electrodeposition from hexachloroplatinate solution. Composition, thickness and substrate dependence. *J. Alloys Compd.* **2017**, *718*, 319–325. [CrossRef]

48. Khurshid, H.; Yoosuf, R.; Issa, B.A.; Attaelmanan, A.G.; Hadjipanayis, G. Tuning Easy Magnetization Direction and Magnetostatic Interactions in High Aspect Ratio Nanowires. *Nanomaterials* **2021**, *11*, 3042. [CrossRef]

49. Cho, J.U.; Wu, J.-H.; Min, J.H.; Ko, S.P.; Soh, J.Y.; Liu, Q.X.; Kim, Y.K. Control of magnetic anisotropy of Co nanowires. *J. Magn. Magn. Mater.* **2006**, *303*, 281. [CrossRef]